Eur. Phys. J. B **3**, 225–236 (1998)

THE EUROPEAN PHYSICAL JOURNAL B

Crystalline structures and phase transition of the ferroelectric P(VDF-TrFE) copolymers, a neutron diffraction study

E. Bellet-Amalric[1,a] and J.F. Legrand[2,b]

[1] Institut Laue-Langevin, BP 156, 38042 Grenoble Cedex, France
[2] Laboratoire de Spectrométrie Physique, Université Joseph Fourier, Grenoble I, BP 87, 38402 Saint Martin d'Hères Cedex, France

Received: 1 March 1996 / Revised: 23 December 1996 and 16 May 1997 / Accepted: 20 February 1998

Abstract. Neutron investigations have been performed in order to study the crystalline structure of the ferroelectric and paraelectric phases of random copolymers of vinylidene fluoride and trifluoroethylene P(VDF-TrFE) and to investigate the influence of co-monomer composition. Structural information in the crystal is essential to understand the mechanism of the phase transition. In the ferroelectric phase, the increase of TrFE content from 20% to 40% clearly affects the crystalline order and leads to an anisotropic expansion of the lattice. At high temperature, complementary studies of diffraction and diffuse scattering, on oriented and deuterated samples, allow us to specify a structural description of the highly disordered paraelectric phase and to propose a model describing the conformational disorder of the chain. From these results we present a thermodynamical analysis of the ferroelectric to paraelectric transition based on the Landau theory which enables to evaluate the different energetic contributions to the structural instability in the crystalline regions of the polymer.

PACS. 61.12.-q Neutron diffraction and scattering – 61.50.Ks Crystallographic aspects of phase transformations; pressure effects – 77.80.Bh Phase transitions and Curie point

1 Introduction

Polyvinylidene fluoride (PVDF) or -$(CH_2$-$CF_2)_n$- and its copolymers with trifluoroethylene (TrFE) or -(CHF-CF_2)- have been the subject of much scientific and technological research due to their piezoelectric and pyroelectric effects [1,2].

These exceptional properties, observed in very few polymeric materials, are based on the presence of a crystalline ferroelectric phase. The polymers are semi-crystalline with a degree of crystallinity ranging from 50 to 80% and should be considered as intrinsically composite: the small ferroelectric crystallites of about 300 Å thickness are embedded in an amorphous matrix. For P(VDF-TrFE) copolymers with VDF content ranging from 65 to 80% the crystalline phase exhibits a clear ferroelectric transition upon heating above room temperature [3]. The Curie Temperature T_C is equal to 380 K for the 65/35 mol% copolymer; it increases with the TrFE contents and eventually merges with the melting point T_M for approximately the 82/18 mol% copolymer.

While the structure of the ferroelectric β-phase of PVDF has been extensively investigated [2,4–8], no precise study exists for the crystal structures of the P(VDF-TrFE) copolymers. The low temperature ferroelectric phase is generally considered to have the same orthorhombic lattice (space group $Cm2m$) as PVDF but with slightly expanded lattice parameters [3,9]. Indeed, if only the similar Van der Waals radii of hydrogen and fluorine atoms is considered, the random substitution of H by F is supposed to introduce little perturbation in the chain structure. On the other hand, the important effect of this substitution on the Curie temperature suggests a noticeable change of the ferroelectric structure.

The structure of the high temperature paraelectric phase $T_C < T < T_M$ has never been clearly described due to its highly disordered nature. Nuclear magnetic resonance (n.m.r.) and Raman experiments have shown that the polymer chains are composed of random sequences of TT, TG and TG^- conformations with large amplitude motion around the chain axis [10,11]. The lattice is hexagonal (space group $6/mmm$) with the six fold axis along the average chain axis [12].

In these polymers the dipolar energy, responsible for the occurrence of the ferroelectric order, is of the order of k_BT_C per monomer [13,14]. The VDF content, which controls the value of the spontaneous polarisation, is thus an essential parameter in determining the stability of the ferroelectric structure.

[a] e-mail: amalric@ill.fr
[b] *Present address*: DRFMC/SI3M, CEA Grenoble, 17 rue des Martyrs, 38054 Grenoble Cedex, France

The present work was undertaken in order to analyse the effect of co-monomer composition on the ferroelectric and paraelectric crystalline phases. Due to the composite nature of the materials, macroscopic scale experiments (*e.g.* DSC, dielectric or specific volume measurements) mix the contributions of the crystalline and amorphous regions. We have performed diffraction experiments (mainly neutrons) which provide information on the crystalline phase alone as the diffuse scattering from the amorphous regions can be easily separated.

2 Experimental

The hydrogenated specimens used in this study were random P(VDF-TrFE) copolymers of compositions 70/30, 80/20 and 60/40 mol% with molecular weight $\overline{M}_n$ and polydispersity $\overline{M}_w/\overline{M}_n \cong 2$ [15]. The samples were supplied by Atochem Company, France. For the structural analysis of the disordered paraelectric phase, a deuterated specimen of 70/30 mol% P(VDF-TrFE), synthesised at A.T. & T. Bell Labs [16] was used.

Two kinds of samples were prepared for the neutron diffraction measurements:

i) unoriented (powder) samples: the raw material was melted in a cylindrical vanadium container of 40 μm wall thickness almost transparent to neutrons (5 mm in diameter and 60 mm in length). Such a preparation is considered to have no effect on the orientation of the sample (powder symmetry maintained). All the samples were annealed at 400 K for about one hour in order to remove any possible residual stress. Additionally it has been shown that after this thermal treatment the degree of crystallinity reaches 80% at room temperature (in the ferroelectric phase) [17,18].

ii) oriented samples: obtained by rolling quenched crystallised plates at 340 K with a draw ratio of about 3.5/1. Such a technique permits only a partial orientation of the chain axis which can be characterised by the measurement of the birefringence. For the deuterated sample, after a first temperature cycle up to 410 K for annealing, we have found $\Delta n = 0.041$ in the ferroelectric phase at 300 K and $\Delta n = 0.043$ in the paraelectric phase at 380 K. Following the results of Krüger *et al.* [19], this reveals a high degree of crystallinity of the sample (ca. 80%) together with a Hermans orientation parameter of ca. 0.7 for the crystalline phase.

The diffraction experiments were performed at the Institut Laue-Langevin using the high flux powder diffractometer D20 and the polarised neutron diffractometer D7.

For hydrogenated materials, the large neutron incoherent cross section of ^{1}H produces a high incoherent background. For highly disordered structures giving diffuse scattering, as for the paraelectric phase, it is therefore necessary to use deuterated samples (the ^{2}H nuclei scatter mainly coherently). Further reduction of the incoherent signal is achieved by means of polarisation analysis of the scattered beam.

For the experiments on the instrument D20 the incoming neutron beam had a wavelength of 2.41 ± 0.01 Å. The instrument is equipped with a multielectrode position sensitive ^{3}He detector which covers an angular range of 12.6 degrees (126 channels). Broader angular ranges were obtained by scanning the multidetector by steps of $\Delta(2\theta) = 3$ degrees and re-grouping the data into a single file (for more details see [20]). For high temperature measurements the sample was placed in a cryo-furnace (1.5 K-600 K) and the temperature of the sample was measured using a rhodium-iron resistor.

The instrument D7 [21] allows separation of the coherent and incoherent diffuse scattering by polarisation analysis of the neutron spin. A focusing triple graphite monochromator provides a wavelength of 5.7 Å or 3.1 Å with $\Delta\lambda/\lambda \cong 10^{-2}$. Spin analysis of the scattered beam is done using a supermirror polarizer, a "Mezei flipper" (spin flip of 180°) and supermirror analyzers. Four banks, of 8 analyzers and ^{3}He detectors (each covering 2 degrees and separated by 6 degrees) can be moved around the sample axis (radius of 1.5 m) in the horizontal plane. The sample was placed with the draw direction (**c** axis) horizontal and rotated around the vertical axis (ω-scans) by steps of 5 degrees, in order to explore the $(h0l)$ plane of the reciprocal space (accordingly the data were recorded along Ewald circles).

For each ω-angle the intensity was measured with and without spin-flip (respectively I_{FL} and I_{NFL}). Such a measurement allows separation of the coherent and the incoherent scattering using the following relations:

$$I_{NFL} = I_{coherent} + 1/3 I_{incoherent}$$
$$I_{FL} = 2/3 I_{incoherent}.$$

In this kind of analysis, the absolute coherent scattering may be determined from the calculated incoherent intensity, which only depends on the composition of the sample.

3 Results

Figures 1a, b, c show neutron powder diffraction patterns in the ferroelectric phase, for three copolymers of different compositions, recorded at room temperature over a broad Q-range [0.8-4.4 Å^{-1}].

As for other semi-crystalline polymers the number of observed Bragg reflections is limited (a principal peak and 4 other peaks of much lower intensity). This is attributed to structural disorder in the crystallites and to thermal fluctuations (Debye Waller factor). Another characteristic is the noticeable width ΔQ of the peaks which is mainly due to Scherrer broadening $\Delta Q \approx 1.8\pi/L$, where L is the coherent size of the crystalline lamellae [17].

For the three copolymers the indexation of the Bragg reflections was done according to the orthorhombic symmetry group $Cm2m$. The systematic absence of the $(hk1)$ reflections with $h + k = 2n$, characteristic of a centred lattice, is observed. Each observed peak consists of two or more overlapping Bragg reflections due to the pseudo-hexagonal nature of the structure. This gives rise to additional broadening of the peaks.

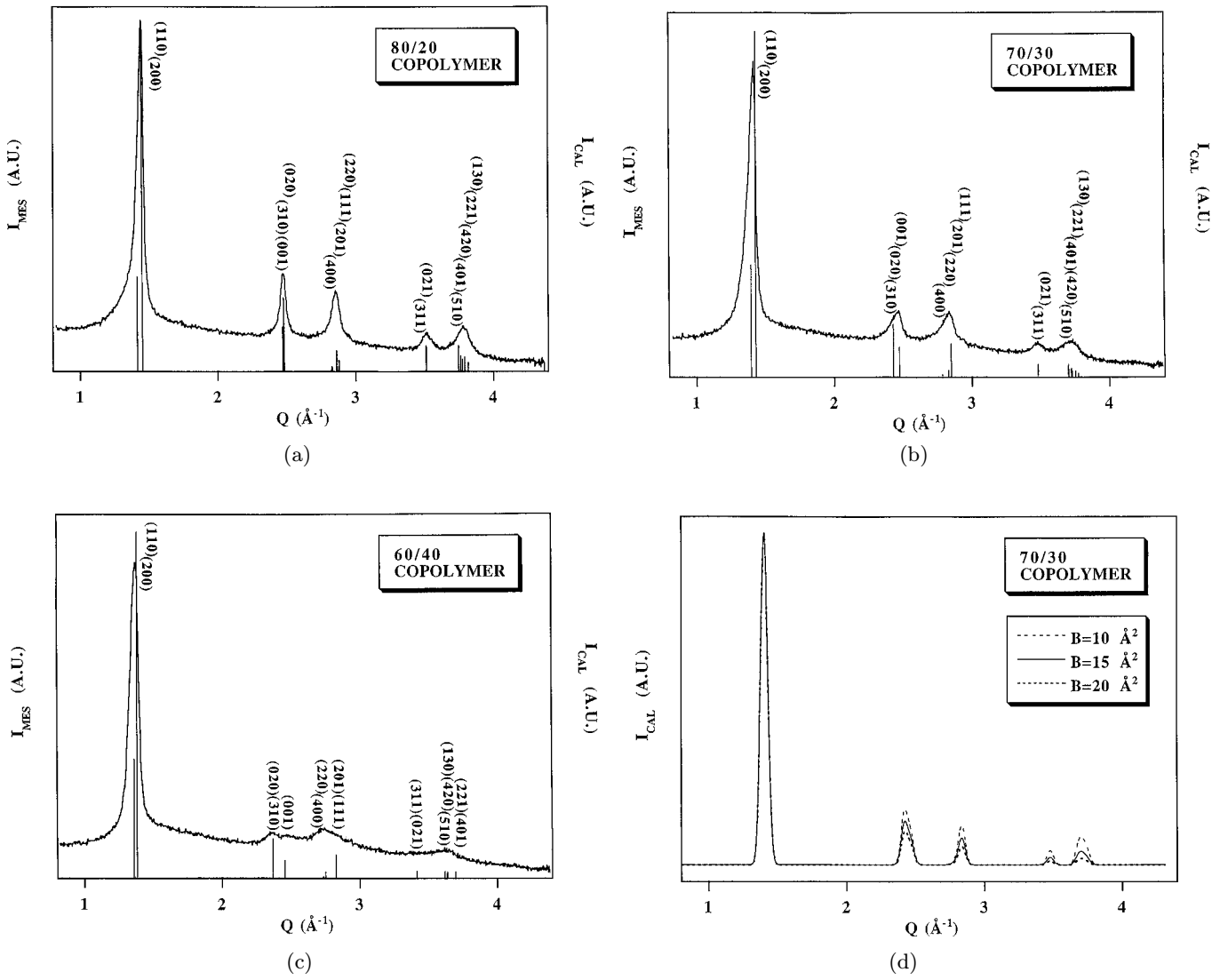

Fig. 1. (a, b, c) Neutron powder diffraction patterns in the Q-range [0.8, 4.4 Å^{-1}], for the ferroelectric phase of respectively the 80/20, 70/30 and 60/40 mol% copolymers. The three plots are shown with the same scale. The indexation was done according to the orthorhombic symmetry group $Cm2m$. For each Bragg reflection, the calculated intensity is represented by means of a bar graphics (the calculations were performed using the following temperature factors: $B = 10$, 15 and 20 Å^2 respectively for the 80/20, 70/30 and 60/40 copolymers). (d) Effect of the temperature factor B on the simulated powder diffraction pattern of the 70/30 mol% copolymer ferroelectric phase. All the calculations were performed with the program LAZY V 1.2 [27].

A comparison of the three powder diffraction patterns reveals that, while increasing the TrFE content, all the peaks, except the (001), are shifted towards lower Q values. This corresponds to an expansion of the lattice along the **a** and **b** directions and explains the accidental superposition of the (001) and ((310) + (020)) reflections for the 80/20 copolymer. Moreover the intensity of the high order reflections decreases from the 80/20 to the 60/40 copolymer. The analysis of the width shows that this is partly due to the decrease of the coherent crystal size but, as will be discussed below, an increasing Debye Waller factor should also be taken into account.

In the paraelectric phase (at 380 K) the powder diffraction patterns show one intense Bragg reflection and three others which are hardly visible (Fig. 2). For the sake of simplicity we use for the hexagonal structure the same indexation as in the ferroelectric phase (centred orthorhombic with $a = b\sqrt{3}$). Two types of Bragg reflections are observed: the ($hk0$) ones very narrow and the (001) very broad; all the other ($hk1$) reflections of the ferroelectric phase have disappeared. In Figure 2 we present only the 70/30 mol% copolymer since in the paraelectric phase the diffraction patterns of the three copolymers do not show any significant difference.

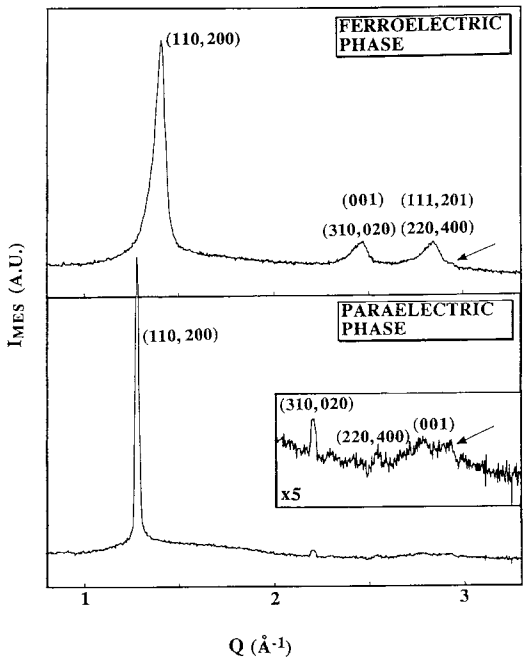

Fig. 2. Neutron powder diffraction patterns of the 70/30 copolymer in the paraelectric phase (380 K) and in the ferroelectric phase (300 K). The two plots are shown with the same scale. The arrow shows the position of the vanadium peak (from the sample container).

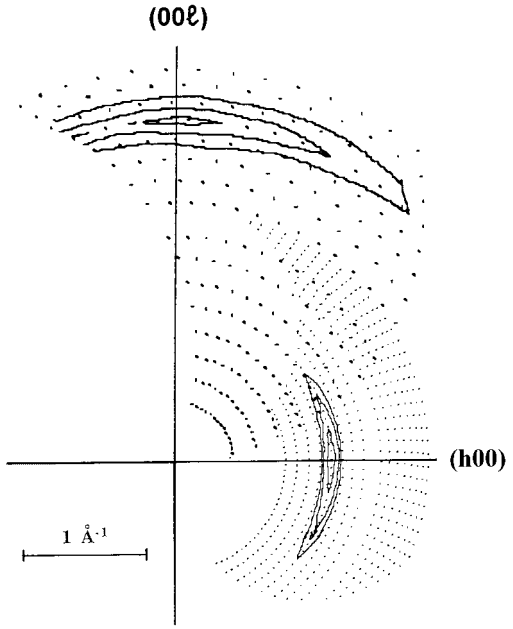

Fig. 3. Contour plots of the coherent diffuse scattering of the paraelectric phase (380 K) in the $(h0l)$ plane (in absolute units). We also show the points representing the reciprocal space which have been explored around the (200) reflection with a wavelength of 5.7 Å, and around the (001) reflection with a wavelength of 3.1 Å. Contour lines correspond to the following values of the differential cross-section: 80, 40 and 20 barn/steradian for the (200) reflection, 10, 7 and 4 barn/steradian for the (001) reflection.

As the powder diffractograms provide very little information on the structure of the paraelectric phase we have studied the time-average structure (Bragg peaks) and the correlated motions of the chains (coherent diffuse scattering) using a deuterated and oriented sample. The total coherent scattering in the $(h0l)$ plane is represented in Figure 3. Two Bragg peaks are observed: the narrow (200) reflection around $Q_x = 1.30$ Å^{-1} and the broad and much weaker (001) reflection around $Q_z = 2.75$ Å^{-1}. The scattering profile of the (001) reflection along the $(00l)$ direction reveals an important asymmetry of the peak which presents a tail towards large Q values.

For the $(hk0)$ reflections the extension of the diffuse scattering along an arc of circle can be attributed to the texture of the sample. The half width of the (200) rocking-curve is 21 degrees and corresponds to a Hermans orientation parameter of the crystalline phase $P_2^c = 0.7$ consistent with the measured birefringence [17]. However, the half width of the (001) rocking-curve (28 degrees) is broader than expected from the sample texture and this may be attributed to a diffuse extension of the (001) reflection in the $(hk1)$ plane.

4 Discussion

4.1 Paraelectric phase

For the time-averaged structure of the chain, in the paraelectric phase, the hexagonal lattice parameter a can be accurately deduced from the (200) reflection in the powder diffractogram. For the 70/30 copolymer we obtain a value of 9.86 Å at 380 K which yields an interchain distance of 5.69 Å (see Tab. 1). However, along the chain axis the lattice parameter c (2.30 Å for the three copolymers) can only be determined on highly oriented samples as we will discuss later. The change in TrFE content does not modify the structure very much and the volume of the lattice remains almost unchanged. This can be understood by taking into account the disordered nature of the paraelectric phase which is insensitive to the substitution of some hydrogen atoms by fluorine atoms.

From a dynamical point of view, the diffuse character of the (001) reflection as well as the disappearance of the other $(hk1)$ reflections can be interpreted by considering the large amplitude motions of adjacent chains in the high temperature phase. Incoherent quasi-elastic neutron scattering experiments, which probe the displacements of the individual protons associated with the conformational changes of the chains, have revealed that each proton undergoes diffusive motions inside a restricted volume (at 387 K this volume corresponds to a cylinder of about 4 Å of diameter and 3 Å height along the chain axis) [11].

Due to such motions, the adjacent chain segments can hardly be correlated along the **c** axis and this is confirmed

Table 1. Ferroelectric and Paraelectric lattice parameters, volume and density of the lattice for the three copolymers. For the ferroelectric phase the orthorhombic deformation ($H = \frac{a}{b\sqrt{3}} - 1$) is also calculated. The results corresponding to the PVDF [6] are added for comparison.

	PVDF	80/20	70/30	60/40 polarised	*60/40 unpolarised*
Ferroelectric Phase (300 K)					
a (Å)	8.58	8.9	9.05	9.2	*9.2*
b (Å)	4.91	5.05	5.12	5.18	*5.3*
c (Å)	2.560	2.550	2.550	2.55	*2.550*
Volume (Å^3)	107.8	114.6	118.2	121.5	*124.8*
Density	1.972	1.960	1.954	1.947	*1.896*
H (%)	0.9%	1.7%	2.0%	2.5%	*0.2%*
Paraelectric Phase (380 K)					
a (Å)	—	9.80	9.86	9.86	
c (Å)	—	2.30	2.30	2.30	
Volume (Å^3)	—	127.5	129.1	129.1	
Density	—	1.762	1.786	1.833	

by our diffraction results:

i) only the projection of the structure in the basal plane is well ordered and yields to narrow ($hk0$) Bragg peaks;
ii) all the other (hkl) reflections ($l \neq 0$) disappear and are replaced by diffuse scattering discs around the ($00l$) nodes which correspond to the structure factor of the isolated chain [22].

Two models have been proposed for the chain structure and its dynamical disorder in the paraelectric phase:

i) a 3/1 helical conformation with kink-3-bond hindered reorientations [23].
ii) a random combination of rotational isomeric sequences of TG, TG$^-$, T$_3$G, and T$_3$G$^-$ [24].

The first model is neither consistent with the diameter of the average cylindrical volume explored by the protons [11], nor with the high conformational disorder expected from the large entropy change at the ferroelectric transition ($\Delta s = 9 \times 10^{-2}$ Jg^{-1}K^{-1} for the 70/30 copolymer [20]). In the second model there is not enough structural information for the comparison with either the incoherent scattering or the coherent diffraction results.

We propose a more detailed approach which takes into account the conformational disorder of the chain inside a restricted volume: the instantaneous conformation of the polymer chain is described by a random sequence of TT, TG and TG$^-$ conformations generated over 6 neighbouring sites around the mean chain axis. Using a diamond lattice model [15] two different directions may be considered (with a 2.3 Å mean repeat distance along the chain axis). The two models are displayed in Figures 4a and b.

i) Model A: (along the (111) direction of the diamond lattice) the 6 possible sites for the carbon atoms are distributed at the edges of two inscribed triangles. Each next sequence has two possible conformations. The conformational entropy per mole of monomers is then $\Delta S \approx R \ln 2$ which corresponds to $\Delta s = 8.4 \times 10^{-2}$ Jg^{-1}K^{-1} (for the 70/30 composition); of the same order of magnitude as the experimental values given above.
ii) Model B: (along the (110) direction of the diamond lattice) the 6 possible sites are distributed at the edges of two connected crosses. Only half of the next chain segments have two possible conformations, the calculated conformational entropy ($\Delta s = 4.2 \times 10^{-2}$ Jg^{-1}K^{-1} for the 70/30 composition) is lower than experimentally observed.

In both cases the dynamical disorder may be described by fast hindered reorientations of chain segments or by 3-bonds crankshafts.

The structure factor of such a dynamically disordered chain, whose time-average structure has a C_∞ symmetry around the chain axis, can be expressed in terms of the Bessel function J_0 by:

$$F(Q_R) = \sum_{atom\ j} f_j J_0(Q_R r_j) \exp\left(\frac{2i\pi l z_j}{c}\right)$$

where

- Q_R is the radial coordinate in the reciprocal space,
- f_j is the atomic scattering factor of the jth atom (for neutrons),
- (r_j, θ_j, z_j) are the cylindrical coordinates of the jth atom,
- c is the periodicity along the z axis,
- $l = 0$ for the ($hk0$) plane,

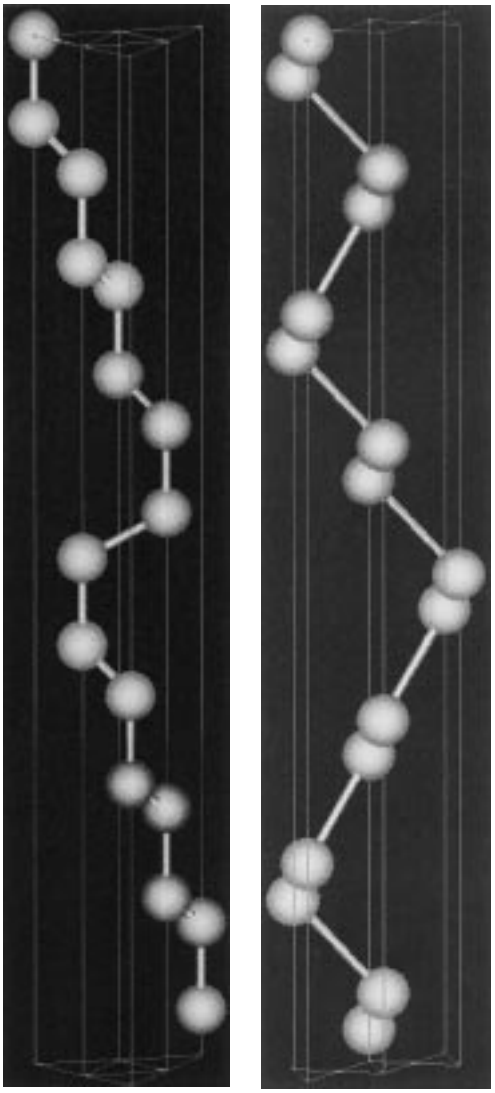

(a) (b)

Fig. 4. Schematic representation of one instantaneous polymer chain in the paraelectric phase. The chain can explore 6 neighbouring positions and is formed by a random mixture of TT, TG and TG^- conformation. Model A: The 6-sites are distributed over two inscribed equilateral triangles, each next sequence has two possible conformations. The figure corresponds to the sequence $TGTG^-TG^-TGTGTT$; Model B: The 6-sites are distributed at the edges of two attached crosses, each other sequence has two possible conformations. The figure corresponds to the sequence $TGTG^-T_3G\ T_3G^-TG$.

- $l = 1$ for the $(hk1)$ plane,
- the sum is made over all the atoms j with $0 \leq z_j < c$ [22].

The calculation was achieved for $l = 0$ and $l = 1$ using the following molecular parameters: for the bond lengths CC = 1.54 Å, CF = 1.36 Å, CH = 1.09 Å, and for the bond angles CCC = 117°, HCH = 110°, FCF = 103°, CCH = CCF = 110°.

Table 2. Calculated neutron diffraction intensities $I_{cal(hk0)} = (F_{C(kh0)})^2 \exp\left(\frac{-Q^2B}{16\pi^2}\right)$ for the two different chain structure in the paraelectric phase. The results are normalised to the intensity of the (110, 200) reflection and were obtained for an isotropic temperature factor $B = 15$ Å^2. For Model B we include also the intensities for $B = 30$ Å^2. The experimental intensities corresponding to a powder sample have been corrected for the geometric Lorentz Factor $L(\theta) = 1/\sin^2(\theta_{(hkl)})\cos(\theta_{(hkl)})$ where $2\theta_{(hkl)}$ is the diffraction angle.

Reflections	Model A	Model B		Experiment
	$B = 15$ Å^2	$B = 15$ Å^2	$B = 30$ Å^2	
(110, 200)	1000	1000	1000	1000
(310, 020)	9	105	75	75
(220, 400)	5.5	70	42	30

The calculated intensities in the $(hk0)$ plane are compared in Table 2 with the experimental ones obtained from the powder measurements. The results were first calculated for a temperature factor $B = 15$ Å^2, the same value as obtained for the ferroelectric phase of the 70/30 copolymer (see Sect. 4.2) ($B = 8\pi^2\langle\Delta u_j^2\rangle$, where Δu_j are the lattice vibrations of the j atom). For Model A the intensities are lower than the experimental one, but the positions of the (310) and (400) Bragg peaks are very close to the first zero of the calculated structure factor and therefore depend very much on the molecular parameters of the model (*e.g.* distortions). For Model B the intensities are higher than the experimental ones, but one must also consider that in such a disordered structure the Debye Waller factor may be much higher. A better agreement with the experimental intensities was obtained for a temperature factor $B = 30$ Å^2 (see Tab. 2), a comparable value was suggested by Renault *et al.* [25] for an analogous rotator phase as observed in monolayers of aliphatic alcohols.

The same structure factor calculation in the $(hk1)$ plane gives the average radius of the (001) diffuse disc scatter by a crystal ($\sigma = 0.72$ Å^{-1} for both models), a small value compared with the extension of the coherent diffuse scattering shown in Figure 3. This is attributed to the texture of the sample which can be simulated by integrating the calculated intensity profile of one crystallite (disc of radius σ and thickness α) over all possible orientations with respect to the $(00l)$ axis. A uniaxial orientation distribution was taken from the texture analysis of the (200) reflection.

Two important experimental features were compared to the calculated results: the width and the asymmetry of the (001) reflection along the Q_z direction. The best agreement was found for $\sigma = 1$ Å^{-1} and $\alpha = 0.08$ Å^{-1}. The α value corresponds to a correlation length of about 70 Å along the chain axis, and the σ value gives a half-width of the (001) rocking-curve of 23 degrees. This result, which arises from the convolution of the radius of the disc with the orientation distribution of the c-axes, is unexpectedly smaller than

the experimental one (28 degrees), and this disagreement remains even when considering larger values of the radius σ. It might be attributed to the use of an inadequate orientation distribution (*e.g.* not uniaxial).

The orientation distribution of the lamellae leads to a displacement of the intensity maximum towards higher values of Q_z ($\Delta Q_z = +0.05$ Å^{-1} for the above values of σ and α). This explains why the lattice parameter c can only be measured on highly oriented samples and why the value obtained by Delzenne [9,17] on a powder sample appears to be underestimated.

In conclusion, Model A accounts for the conformational entropy of the paraelectric phase, but its calculated structure factor shows that the range of radial distances explored by the atoms is too large (*e.g.* for the hydrogen atoms they amount to 2.4 Å instead of 2.0 Å [11]). Alternatively, Model B exhibits less conformational entropy but is slightly more compact around the chain axis and thus gives a better agreement with the powder diffraction results. In addition only Model B is consistent with a large temperature factor B as expected for a conformationally disordered structure ("condis" phase [26]). The experimental entropy change at the transition might be attributed not only to the conformational disorder but also to the decrease in the degree of crystallinity (partial melting of about 7% [17]) through the ferroelectric to paraelectric transition. The measured entropy change at the transition would therefore be higher than calculated from the conformational model.

As regards to the effect of co-monomer composition, it is worth noting that, at a given temperature, the structure of the paraelectric phase, its unit cell volume and its entropy are not much sensitive to the TrFE content (Tab. 1), but depend strongly on temperature [20]. The decrease of the enthalpy of transition with increasing the TrFE content [20] can be attributed both, to the increase of the unit cell volume and of the disorder of the ferroelectric structure (Tab. 1), and to the lowering of the transition temperature. The proposed models A and B can be used to describe the structure and the entropy of the paraelectric phase independently of the composition.

4.2 Ferroelectric phase

Structure factor

We have calculated the neutron structure factors in the ferroelectric phase for PVDF and the three copolymers for comparison with the powder diffraction results at room temperature. This has been done using the program LAZY V 1.2 [27].

In a first stage we calculated the intensities for a zigzag chain without orientational disorder. The atomic coordinates determined by Hasegawa *et al.* [6] were used for the PVDF and an isotropic temperature factor corresponding to the value found for the homopolymer ($B = 5$ Å^2) was considered for all the atoms. For the copolymers, two modifications were introduced: i) random substitution of hydrogen atoms by fluorine atoms and ii) correction of the reduced atomic coordinates according to the change of the lattice parameters. For the 60/40 copolymer we have considered the lattice parameters of the non distorted ferroelectric phase (*i.e.* a polarised sample as will be seen below).

The powder intensities calculated for the observable Bragg reflections (taking into account the Lorentz Factor and the multiplicity of each reflection) are listed in Table 3. When considering the same temperature factor $B = 5$ Å^2, it appears that the influence of co-monomer substitution is very small (even on the nearly extinguished reflections); except for the (001) reflection whose intensity clearly decreases with increasing TrFE content. The random introduction of more fluorine affects therefore the order along the chain.

In contrast to the above calculations, the powder diffraction patterns reveal a clear change with composition in the shape and the intensity of the Bragg reflections (see Figs. 1a, b, c). Besides the broadening due to the orthorhombic distortion of the pseudo-hexagonal lattice, one has to consider a disorder of the structure increasing with the TrFE content. Such a disorder can be taken into account, in a first approximation, by an isotropic Debye Waller factor. In a next step, we have compared the experimental diffraction patterns with simulated ones for different isotropic temperature factors B. Figure 1d displays the simulated diffraction patterns of the 70/30 copolymer for three values of the temperature factor $B = 10$, 15 and 20 Å^2. An average coherence length of 70 Å was considered to account for the line width of each Bragg peak (as determined by the average size of the ferroelectric domains [18]).

For the different copolymers the best global agreement is obtained using the following isotropic temperature factors:

$B = 10$ Å^2 for the 80/20 copolymer
$B = 15$ Å^2 for the 70/30 copolymer
$B = 20$ Å^2 for the 60/40 copolymer.

A systematic discrepancy remains for the (310) and (510) reflections for which the calculated intensities are much higher than the experimental ones. This effect has also been observed for the homopolymer PVDF [6]. The difference can be explained by a large positional disorder of the atoms along the **a** direction and could be taken into account by an anisotropic B temperature factor (which would decrease the intensity of all the (hkl) reflections, with $h \gg k$ and $h \gg l$).

The noticeable change of the temperature factor, while incorporating randomly more TrFE monomers, reveals an increasing disorder and distortion of the ferroelectric structure which eventually becomes metastable relative to a low temperature disordered phase (LTD) [20].

Indeed, for the 60/40 copolymer a broad reflection appears around 2.7 Å^{-1} (Fig. 1c) which cannot be indexed in the ferroelectric structure and which arises from the coexistence of the LTD phase with the ferroelectric phase.

Table 3. Calculated neutron diffraction intensities using the program LAZY V 2.1 [27] for different co-monomer compositions. The intensities $I_{cal}(hkl)$ include the geometric Lorentz Factor $L(\theta) = 1/\sin^2(\theta_{(hkl)})\cos(\theta_{(hkl)})$, the diffraction angle $(\theta_{(hkl)})$ and the multiplicity $m_{(hkl)}$ of the (hkl) reflection. The results are normalised to the intensity of the (110) reflection and were obtained for an isotropic temperature factor $B = 5$ Å^2. The $Q_{(hkl)}$ values corresponding to the 70/30 copolymer are indicated as a guide.

Reflections	Q(70/30)	I_{cal} (PVDF)	I_{cal} (80/20)	I_{cal} (70/30)	I_{cal} (60/40)
(110)	*1.41*	1000	1000	1000	1000
(200)	*1.38*	242	294	334	366
(001)	*2.46*	203	165	148	132
(310)	*2.42*	305	275	264	254
(020)	*2.45*	2	2	4	6
(111)	*2.84*	128	187	209	239
(201)	*2.83*	2	5	5	6
(400)	*2.78*	27	17	13	10
(220)	*2.82*	45	46	44	44
(021)	*3.48*	150	135	129	124
(311)	*3.45*	3	0	0	0
(510)	*3.68*	143	153	152	150
(420)	*3.71*	44	75	93	112
(130)	*3.75*	58	53	48	43
(401)	*3.71*	114	95	85	76
(221)	*3.74*	87	86	86	88

Lattice parameters

From the powder diffraction patterns, due to the accidental superposition of the (001) and ((310) + (020)) reflections, it is impossible to determine precisely the lattice parameter c, while for oriented samples, the diffraction of the [001] and [310 + 020] planes correspond to different orientations: along the meridian or in the equatorial directions. Additional high resolution diffraction experiments were performed using oriented samples of PVDF and of the three copolymers. As predicted by the calculation (see Tab. 3) we observe a huge decrease of the (001) Bragg peak intensity when increasing the TrFE content. The values obtained for the lattice parameter c are:

$c = 2.560 \pm 0.001$ Å for the PVDF

$c = 2.550 \pm 0.003$ Å for the three copolymers 80/20, 70/30 and 60/40.

The small difference of the c parameter between the PVDF and the 70/30 mol% copolymers has already been reported [3] and is opposite to what is expected from the steric hindrance of the fluorine atoms. This modification could be explained by the slight distortion of the chains with respect to the planar zig-zag conformation (of about ±7 degrees as suggested for PVDF [6]), or alternatively by a slight distortion of the lattice (monoclinic distortion of about 5 degrees as suggested for the 55/45 mol% copolymer [3]).

Using the above values of the c lattice parameter and the calculated intensities, we could refine the others lattice parameters for the three copolymers. For the 60/40 copolymer we have compared a polarised sample (with ferroelectric phase alone) and an unpolarised sample (with coexistence of the ferroelectric phase with the LTD phase [20]). The results are given in Table 1 and the values corresponding to PVDF [6] have been added for comparison.

Several effects of the co-monomer composition are revealed:

- The increase of the lattice volume: while the c lattice parameter remains almost constant, the values of the a and b lattice parameters increase with the TrFE content. However, the volume increase being larger than the increase of mass (due to the substitution of hydrogen by fluorine atoms) the density of the crystalline phase decreases. This result confirms the higher disorder of the crystalline structure compared to that of the homopolymer.
- The anisotropic expansion of the lattice: the evolution of the lattice parameters a and $b\sqrt{3}$ with the co-monomer composition are shown in Figure 5. In the absence of phase coexistence both lattice parameters increase linearly with the TrFE content but the volume change is anisotropic, the increase of the a parameter being larger than that of the $b\sqrt{3}$ parameter. The pseudo-hexagonal nature of the lattice cell, which can be described by an orthorhombic

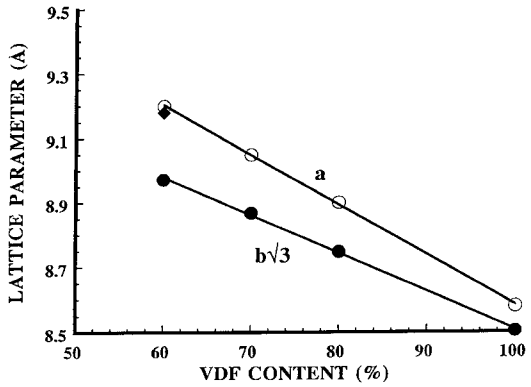

Fig. 5. Evolution of the lattice parameters a (○) and $b\sqrt{3}$ (●) with the composition. For the 60/40 copolymer the two values of $b\sqrt{3}$ correspond to the ferroelectric phase alone (●) and to the coexistence of the ferroelectric phase with the LTD phase (⧫).

deformation $H = \dfrac{a}{b\sqrt{3}} - 1$, increases with the TrFE content (see Tab. 1). This result is contrary to what would be expected from the effect of electrostriction (contraction along the polar **b** axis). For the copolymers, the spontaneous polarisation being lower, the lattice parameter $b\sqrt{3}$ should increase more than the a lattice parameter. The larger change of the a lattice parameter can again be related to the anisotropic atomic position disorder due to the deflection of the chain in the a direction.

In the case of phase coexistence (60/40 copolymer), the ferroelectric structure is strained towards a nearly hexagonal symmetry. But as the coexisting phases are expanded, the application of an external pressure as well as the application of an electric field (polarisation of the sample) [28], is able to restore the ferroelectric structure [20].

4.3 Ferroelectric transition and Landau free energy

The accurate determination of the structural parameters in the ordered and disordered phases permits a renewed discussion of the thermodynamics of the ferroelectric phase transition, based on the properties of the crystalline phase alone. Indeed, in an inhomogeneous semicrystalline polymer, only averaged order parameters can be measured from macroscopic measurements, while from our structural studies, the microscopic characteristics of the crystalline phase itself have been determined.

We will consider a Landau type of expansion of the free energy F in terms of the spontaneous polarisation along the crystal b axis ($P = P_y$) and of the components of the lattice strains tensor along the 3 crystal axes (u_{xx}, u_{yy} and u_{zz}). The aim of such an approach is to estimate the two different energies (dielectric and elastic) contributing to the equation of state of the ferroelectric phase and also to evaluate the effect of the coupling between polarization and lattice strain on the temperature dependence of the order parameter. In this section we will not discuss the details of the phase transformation in the vicinity of T_C but instead the overall behaviour of the transition [29].

Table 4. Effect of composition on: the average dipole moment of a monomer $\overline{\mu}$, the double of the primitive cell volume $2\nu_{0K}$ extrapolated to 0 K, the saturation polarisation P_0, the predicted Curie temperature T_0, the experimental transition temperature upon heating T_{c+} [20] and the lattice strains u_{xx}, u_{yy}, u_{zz} at T_{c+} derived from the temperature dependence of the lattice parameters [20].

	PVDF	80/20	70/30	60/40
$\overline{\mu}$ (10^{-30} Cm)	7.0	6.3	6.0	5.6
$2\nu_{0K}$ (Å^3)	102	107	112	115
P_0 (mC/m^2)	137	118	106	97
T_0 (K)	630	480	410	350
T_{c+} (K)	-	404	362	338
u_{xx} (T_{c+})	-	−8.8%	−7.2%	−4.9%
u_{yy} (T_{c+})	-	−10.3%	−9.0%	−7.4%
u_{zz} (T_{c+})	-	+10.9%	+10.9%	+10.9%

The Landau approach, originally developed for second order transitions, can be extended to first order ones for structural changes with a group/subgroup relation as in this case. For the symmetry change of the copolymer transition ($Cm2m \rightarrow P6/mmm$), the free energy of the crystalline phase can be expanded taking into account the electrostrictive coupling between the polarization P and the lattice strains u_{ii}.

$$\begin{aligned} F(P,u,T) = {} & \alpha(T-T_0)P^2/2 + \beta P^4/4 + \gamma P^6/6 \\ & + g_{12}u_{xx}P^2 + g_{22}u_{yy}P^2 + g_{32}u_{zz}P^2 \\ & + C_{11}u_{xx}^2/2 + C_{11}u_{yy}^2/2 + C_{33}u_{zz}^2/2 \\ & + C_{12}u_{xx}u_{yy} + C_{13}u_{xx}u_{zz} + C_{13}u_{yy}u_{zz}. \end{aligned} \quad (1)$$

In the above expression T_0 is the fixed point of the Curie-Weiss law in the paraelectric phase, g_{ij} are the electrostriction coefficients, C_{ij} are the components of the elastic stiffness tensor of the prototype phase (paraelectric) and α, β and γ are the Landau coefficients. We define the lattice strains by the difference between the ferroelectric and the paraelectric lattice parameters:

$$u_{xx} = \frac{(a_{ferro} - a_{para})}{a_{para}} \qquad u_{yy} = \frac{(b_{ferro} - b_{para})}{b_{para}}$$
$$u_{zz} = \frac{(c_{ferro} - c_{para})}{c_{para}}$$

where the paraelectric unit cell is taken at the transition temperature. According to the experimental results (see Tab. 1) u_{xx} and u_{yy} are negative while u_{zz} is positive (Tab. 4).

Derivations of (1) with respect to u_{xx}, u_{yy} and u_{zz} yield the following linear relation, between the lattice

strains and the square of the spontaneous polarisation in the ordered ferroelectric phase:

$$\begin{pmatrix} C_{11}\ C_{12}\ C_{13} \\ C_{12}\ C_{11}\ C_{13} \\ C_{13}\ C_{13}\ C_{23} \end{pmatrix} \begin{pmatrix} u_{xx} \\ u_{yy} \\ u_{zz} \end{pmatrix} = -P^2 \begin{pmatrix} g_{12} \\ g_{22} \\ g_{32} \end{pmatrix} \cdot \quad (2)$$

The free energy can thus be re-normalized as:

$$F(\eta, T) = a(T - T_0)\frac{P^2}{2} + \left(\beta - \frac{2G^2}{C}\right)\frac{P^4}{4} + \gamma\frac{P^6}{6} \cdot \quad (3)$$

In this expression the coupling with the elastic deformation is expressed by the global electrostrictive term $\frac{2G^2}{C}$ [30] whose effect is to reduce the coefficient β and eventually to transform a second order phase transition with $\beta > 0$ into a first order one, with a re-normalized coefficient: $\beta^* = \left(\beta - \frac{2G^2}{C}\right) < 0$.

The free energy expansion can also be written in terms of the order parameter $\eta = P/P_0$ where P and P_0 are respectively the spontaneous and the saturated polarisations:

$$F(\eta, T) = \alpha P_0^2 (T - T_0)\frac{\eta^2}{2} + \left(\beta - \frac{2G^2}{C}\right) P_0^4 \frac{\eta^4}{4} + \gamma P_0^6 \frac{\eta^6}{6} \cdot \quad (4)$$

With the aim of estimating and comparing the *orders of magnitude* of the different interactions contributing to the phase transition, we have evaluated, from the available experimental data, approximate values of most coefficients of the free energy expansion (4).

Electrostatic contribution to the free energy

• The saturation polarisation $P_0 = \frac{\overline{\mu}}{\nu_{0K}}$ is obtained from the primitive cell volume ν_{0K} (values from Tab. 1 extrapolated to 0 K using linear thermal expansion coefficients [18]) and from the average dipole moment of a monomer: $\overline{\mu} = \mu_0\left(1 - \frac{x}{2}\right)$ (with μ_0 the dipole moment of CH_2-CF_2 and x the CHF-CF_2 content) (Tab. 4). In a first approximation, the equilibrium polarisation is derived from direct summation of the dipole moments without Lorentz field correction [31].

The results of Table 4 reveal that two factors contribute to the decrease of the polarisation (from PVDF to 60/40 copolymer): the reduction of the dipole moment (ca. 65%) and the increase of the cell volume (ca. 35%). The results obtained for P_0 are in agreement with the macroscopic values of the remanent polarisation measured, in semicrystalline samples, taking into account the degree of crystallinity and the texture [13,32].

• As has been shown for a series of ferroelectric crystals, an *ab-initio* evaluation of the Curie temperature T_0 may be obtained from the order of magnitude of the (ferroelectric) dipolar energy W_D using [33]

$$T_0 = \frac{W_D}{k_B} = \frac{\nu_{0K} P_0^2}{k_B}.$$

It is remarkable that the values obtained (Tab. 4) from such a simple prediction of T_0 agree within 20% with the absolute transition temperatures T_{c+} observed for the different co-monomer compositions. This really confirms the dominant role of the dipolar energy in the phase transition mechanism of these ferroelectric polymers.

• The order of magnitude of the α and β coefficients may be obtained following the Bragg Williams approach of an Ising model. From the Hamiltonian $H = \sum_i \sum_j J_{ij} S_i S_j$ (with the pseudo-spin variables S_i, $S_j = \pm 1$), the two first terms of the free energy expansion can be expressed using the dimensionless order parameter $\eta = \frac{\sum_i S_i}{\sum_i |S_i|}$ as:

$$F(\eta, T) = \frac{k_B}{\nu_{0K}}(T - T_0)\frac{\eta^2}{2} + \frac{k_B T}{3\nu_{0K}}\frac{\eta^4}{4} \quad (5)$$

where $T_0 = \frac{2\sum_j J_{ij}}{k_B}$ is the Curie temperature of the pseudo spin system [34]. Comparison with expression (3) gives: $\alpha = \frac{k_B}{\nu_{0K} P_0^2}$ and $\beta = \frac{k_B T}{3\nu_{0K} P_0^4}$.

For the 70/30 mol% copolymer this gives $\alpha = 2.2 \times 10^7\ \mathrm{Nm^2C^{-2}K^{-1}}$ and $\beta \approx 2.6 \times 10^{11}\ \mathrm{Nm^6C^{-4}}$ for $T \approx T_0$.

To summarize these results, the free energy expansion (5) contains two entropic terms whose balance by the pure dipolar contribution would give rise to a second order phase transition at T_0, in the absence of coupling with the lattice strains.

Let us remark that expression (5) is only valid close to the transition. At lower temperature, it is necessary to introduce phenomenologically, as in expression (4), a term of higher order $\gamma P_0^6 \frac{\eta^6}{6}$ which accounts for the saturation of the polarisation.

Elastic contribution to the free energy

• The evaluation of the elastic free energy:

$$\frac{W_{el}}{\nu_{0K}} = \frac{1}{2}\sum_{ij} C_{ij} u_{ii} u_{jj},$$

requires the values for the elastic stiffness coefficients C_{ij} in addition to the elastic strains (Tab. 4). The only available data have been obtained from Brillouin scattering experiments, for the 70/30 mol% copolymer [35]:

$$C_{11} = 5.5\ \mathrm{GPa}$$
$$C_{33} = 8.5\ \mathrm{GPa}$$
$$C_{12} \approx C_{13} \approx 3.5\ \mathrm{GPa}.$$

The values of C_{11} and C_{33} have been measured, in the paraelectric phase, just above the experimental transition temperature upon heating ($T_{c+} = 362$ K [17]). In this high temperature range, the C_{12} and C_{13} coefficients have not been measured but we have estimated the above order of magnitude from comparisons with the ferrolectric phase.

Using these values it is possible to evaluate the elastic energy:

$$\frac{W_{el}}{k_B} = 190 \text{ K}.$$

Such a high value, almost one half of $\frac{W_D}{k_B}$, points out the important role of the elastic energy in the phase transition mechanism. As we will discuss below, its main effect is to renormalize the phase transition towards a first order type.

• Under the assumption of quadratic couplings between P and u_{ii} (*cf.* Eq. (2)) the electrostrictive contribution to the free energy is equal to $-2\frac{W_{el}}{\nu_{0\text{K}}}$. The overall effect in the free energy expansion is thus a negative contribution $-\frac{W_{el}}{\nu_{0\text{K}}}$ which reduces the β coefficient by $\frac{2G^2}{C} = \frac{4W_{el}}{\nu_{0\text{K}} P_0^4}$.

From the above evaluations we get $\frac{2G^2}{C} \approx 1.5 \times 10^{12}$ Nm^6C^{-4}. This order of magnitude estimate yields a large negative value for the renormalized coefficient $\beta^* = \left(\beta - \frac{2G^2}{C}\right) \approx -1.2 \times 10^{12}$ Nm^6C^{-4}. This result indicates that, it is the strong coupling between the polarization and the strains which induces a high first order character for the transition (abrupt discontinuity of the order parameter and broad thermal hysteresis).

• In conclusion, the Landau approach yields to a good evaluation of the electrostatic energy (with a surprisingly good evaluation of the T_0 and P_0 values). With regards to the elastic energy it predicts a first order transition for the 70/30 mol% copolymer but, the value of the coefficient β^* seems overestimated. Indeed, starting from such a high value, it is unlikely that β^* could become positive for copolymers with a TrFE content greater than 40%, whose phase transition appears, experimentally, to be of second order type. With increasing the TrFE content, the decrease of the dipolar energy, as well as the smaller lattice parameter discontinuity, would tend to reduce the electrostrictive coupling but not enough to change the sign of β^*.

The above results point out some limitations of this Landau approach. The large values of the spontaneous strains are much beyond the elastic regime and for a better description of the coupling with the polarization, higher order terms should be included in the free energy expansion. In considering the paraelectric phase as a unique prototype phase for all the compositions, we have neglected the shift of the Curie temperature T_C and therefore the large structural changes of this disordered phase with temperature. Let us recall that the huge thermal expansion of the paraelectric phase [20] suggests a large change of its entropy at T_C.

5 Conclusion

The structure of the two crystalline phases: ferroelectric and paraelectric and the effect of co-monomer composition have been investigated. The different energetic terms contributing to the phase transition in the crystal phase have been evaluated.

While the structure of the low temperature ferroelectric phase of the copolymers has previously been considered to be the same as for the homopolymer PVDF, we have shown that in fact the ferroelectric structure appears to be very sensitive to the composition. Increasing the TrFE content produces an anisotropic expansion of the lattice and induces a distortion of the chain in the **a** direction, *i.e.* perpendicular to the zig-zag plane. Consequently the structural disorder increases. We have described this with an isotropic temperature factor B. More information could be obtained by an analysis of oriented samples taking into account anisotropic B factors, as well as measurements at low temperature in order to separate the static and dynamic contributions to the disorder.

For the paraelectric phase the analysis of the structure reveals no real dependence upon the co-monomer composition. The chains, which are dynamically disordered, occupy cylindrical volumes which are very well ordered in a hexagonal lattice with a lateral coherence length of about 800 Å. This gives rise to very narrow ($hk0$) Bragg peaks. In contrast, the conformational disorder of the chains and the absence of correlation between neighbouring chain segments along the **c** axis, produces a diffuse (001) disc extended along the (q_x, q_y, 1) reciprocal plane.

From complementary results of powder diffraction and diffuse scattering, in the paraelectric phase, we propose two models for the structure of the chain. Both consist of a random mixture of TT, TG and TG^- conformations distributed over 6 neighbouring sites. These simple structural models describe most features of the coherent scattering and give a conformational disorder in reasonable agreement with the large entropy change at the ferro to paraelectric transition.

These new structural results enable us to evaluate the ordering effect of the dipolar and elastic energies as compared to the entropy change at the transition, using a Landau type approach.

The entropy difference at the transition ($S_{para} - S_{ferro}$) decreases with increasing TrFE content. This is attributed to several combined mechanisms:

i) a smaller dipolar energy which lowers the temperature range of stability of the ferroelectric phase,
ii) a smaller elastic energy which reduces the first order character of the transition and which is associated to
iii) a higher entropy S_{ferro} (and specific volume) of the ferroelectric phase due to a higher disorder of the structure, and a smaller entropy S_{para} (and specific volume) of the paraelectric phase at T_c, due to the lowering of the transition temperature.

$$\frac{2G^2}{C} = \frac{2(g_{12}-g_{22})^2(C_{11}C_{33}-C_{13}^2)+2g_{32}^2(C_{11}^2-C_{12}^2)+4(C_{11}-C_{12})(g_{12}g_{22}C_{33}-g_{12}g_{32}C_{13}-g_{22}g_{32}C_{13})}{(C_{11}-C_{12})(C_{11}C_{33}+C_{12}C_{33}-2C_{13}^2)}$$

New information on the structure and phase transition properties of the ferroelectric crystallites in P(VDF-TrFE) copolymers has been presented in this work. A better knowledge of the crystal phase is essential for modelling the composite nature of this semicrystalline material and its thermodynamic properties in relation to the morphology.

It is a pleasure to acknowledge the scientific and technical support of ILL staff and especially O. Schaerpf and P. Convert for their valuable assistance. We also wish to thank J. Lajzerowicz for fruitful discussions. The deuterated sample was kindly supplied by A.J. Lovinger, R.E. Cais and V.H. Schmidt. We are grateful to Atochem Company, France for donating the raw material for all the other samples.

References

1. T.T. Wang, J.M. Herbert, A.M. Glass, *The Applications of Ferroelectric Polymers* (Blackie and Son, Glasgow, 1987).
2. A.J. Lovinger, *Developments in Crystalline Polymers -1* (Applied Science, London, 1982), pp. 195-273.
3. K. Tashiro, K. Takano, M. Kobayashi, Y. Chatani, H. Tadokoro, Ferroelectrics **57**, 297 (1984).
4. Ye.L. Galperin, Yu.V. Stogalin, M.P. Mlenik, Vysokomol. Soed. **7**, 933 (1965).
5. J.B. Lando, H.G. Olf, A. Peterlin, J. Polym. Sci. A-1 **4**, 941 (1966).
6. R. Hasegawa, Y. Takahashi, Y. Chatani, H. Tadokoro, Polym. J. **3**, 600 (1972).
7. N. Takahashi, A. Odajima, Ferroelectrics **32**, 49 (1981).
8. F.J. Baltá Calleja, A. González Arche, T. Ezquerra, C. Santa Cruz, F. Batallán, B. Frick, E. López Cabarcos, Adv. Polym. Sci. **108**, 1 (1993).
9. P. Delzenne, PhD. Thesis (1986), Grenoble Univ., unpublished.
10. K. Tashiro, M. Kobayashi, Phase Trans. **18**, 213 (1984).
11. J.F. Legrand, B. Frick, B. Meurer, V.H. Schmidt, M. Bee, J. Lajzerowicz, Ferroelectrics **109**, 321 (1990).
12. A. Wicker, B. Berge, J. Lajzerowicz, J.F. Legrand, J. Appl. Phys. **66**, 342 (1989).
13. T. Furukawa, Phase Trans. **18**, 143 (1989).
14. B. Daudin, J.F. Legrand, F. Macchi, J. Appl. Phys. **70**, 4037 (1991).
15. J. Hirschinger, B. Meurer, G. Weill, J. Phys. France **50**, 563 and 583 (1989).
16. R.E. Cais, J.M. Kometani, Macromol. **17**, 1887 (1984).
17. C. Bourgaux-Leonard, J.F. Legrand, A. Renault, P. Delzenne, Polymer **32**, 597 (1991).
18. K. Tashiro, R. Tanaka, K. Ushitora, M. Kobayashi, Ferroelectrics **171**, 145 (1995).
19. J.K. Kruger, M. Prechtl, J.C. Wittmann, S. Meyer, J.F. Legrand, G. d'Assenza, J. Polym. Sci. - Part B **31**, 505 (1993).
20. E. Bellet-Amalric, J.F. Legrand, M. Stock-Schweyer, B. Meurer, Polymer **35**, 34 (1994).
21. B. Gabrys, O. Schaerpf, D.G. Pfeiffer, *Physical Chemistry of Ionomers - A Monograph*, edited by S. Schlick (CRC Press, 1996), pp. 57-81.
22. D.W. Hukins, *X-ray Diffraction by Disordered and Ordered Systems* (Pergamon Press, Oxford, 1981), pp. 94-118.
23. C. Perry, E.A. Dratz, Y. Ke, V.H. Schmidt, J.M. Kometani, R.E. Cais, Ferroelectrics **92**, 55 (1989).
24. K. Tashiro, K. Takano, M. Kobayashi, Y. Chatani, H. Tadokoro, Polymer **25**, 195 (1984).
25. A. Renault, J.F. Legrand, B. Berge, M. Goldman, J. Phys. II France **3**, 761 (1993).
26. B. Wunderlich, J. Grebowicz, Adv. Polym. Sci. **60/61**, 1 (1984).
27. K. Yvon, A.W. Hewat, Apple Software.
28. G.T. Davis, T. Furukawa, A.J. Lovinger, M.G. Broadhurst, Macromol. **15**, 329 (1982).
29. One may find in the litterature several papers, based on calorimetric and dielectric measurements, showing that the ferroelectric transition of 70/30 and 75/25 mol% copolymers occur in at least two steps (T.A. Ezquerra, F. Kremer, F.J. Balta-Calleja, E. Lopez Cabarcos, J. Polym. Sci Part B **32**, 1449 (1994); H. Tanaka, H. Yukawa, T. Nishi, Macromol. **21**, 2469 (1988). These effects can be explained by morphological changes inside the semi-crystalline material and are very sensitive to the thermal history of the samples which affect the nucleation and growth of the crystallites. Indeed, papers based on structural studies, reveal no intermediate crystalline structure between the ferroelectric and the paraelectric ones, but show a spreading of the transition temperature T_C over the heterogeneous population of crystallites. The distribution of T_C is strongly dependent on the thermal and electrical history of the sample (G.R. Li, N. Kagami, H. Ohigashi, J. Appl. Phys. **72**, 1056 (1992); K. Tashiro, R. Tanaka, K. Ushitora, M. Kobayashi, Ferroelectrics **171**, 145 (1995) [16]).
30. The exact expression of the electrostrictive term is given by

(see equation above)

31. Calculations of the Lorentz field factor f are very sensitive to the symmetry of the lattice and to the size of the dipoles (K. Koga, H. Ohigashi, J. Appl. Phys. **59**, 2142 (1986)). For β-PVDF a factor $f = 1.85$ is found for cubic lattice and point dipoles (G.T. Broadhurst, G.T. Davis, J.E. McKiney, J. Appl. Phys. **49**, 4992 (1978)) while, for an orthorhombic structure, it is estimated to only $f = 0.98$ (R. Al-Jishi, P.L. Taylor, J. Appl. Phys. **57**, 902 (1985)).
32. J.F. Legrand, J. Lajzerowicz, B. Berge, P. Delzenne, F. Macchi, C. Bourgaux-Leonard, A. Wicker, J.K. Krüger, Ferroelectrics **78**, 151 (1988).
33. J. Lajzerowicz, J.F. Legrand, Phys. Rev. B **17**, 1438 (1978).
34. J.F. Legrand, J. Lajzerowicz, J. Lajzerowicz-Bonneteau, A. Capiomont, J. Phys. France **43**, 1117 (1982).
35. J.K. Kruger, J. Petzelt, J.F. Legrand, Coll. Polym. Sci. **264**, 791 (1986).